Synthesis of a Multinary Nitride, Eu-Doped $CaAlSiN_3$, from Alloy at Low Temperatures

Jinwang Li,*,† Tomoaki Watanabe,†,‡ Naonori Sakamoto,†,§ Hiroshi Wada,△ Tohru Setoyama,△ and Masahiro Yoshimura†

Materials and Structures Laboratory, Tokyo Institute of Technology, 4259 Nagatsuta, Midori, Yokohama 226-8503, Japan, and Mitsubishi Chemical Group Science and Technology Research Center, Inc., 1000 Kamoshida, Aoba, Yokohama 227-8502, Japan

Received June 18, 2007. Revised Manuscript Received January 12, 2008

A multinary nitride, Eu-doped $CaAlSiN_3$, which had previously been synthesized at 1600–1800 °C as a red-emiting phosphor material, was obtained at 500–800 °C via the reaction of a CaAlSi alloy with a low concentration of Eu (composition $Ca_{0.992}Eu_{0.008}AlSi$) in ammonia in the present study. In supercritical ammonia (100 MPa), $CaAlSiN_3$ was formed at temperatures ≥ 500 °C both with and without the addition of sodium amide. The addition of sodium amide significantly facilitated the synthesis and prevented the presence of unreacted silicon, which could be due to the formation of sodium ammonometallates as intermediates in the presence of sodium amide. $CaAlSiN_3$ was synthesized even in an atmospheric ammonia flow, but the crystallinity of the product was rather low. Evidence suggested that $CaAlSiN_3$ was insoluble in the pressurized sodium amide−ammonia medium under the present conditions, and the prolonged reaction of the alloy in ammonia at the $CaAlSiN_3$-forming temperatures (500–800 °C) did not result in an effective improvement of the crystallization. In contrast, well-crystallized samples with plate- and bar-like nanocrystals were synthesized by first converting the alloy at 300–400 °C into sodium ammonometallates and subsequently decomposing the ammonometallates up to 800 °C into $CaAlSiN_3$. The products showed a red emission centered at 630–644 nm at a blue excitation of 460 nm. Instead of using sodium amide, the use of sodium azide, which was converted into sodium amide during heating, led to a product of plate-like crystals with significantly reduced oxide (oxide-free in the XRD spectrum) but did not result in an improved light emission. The size and lattice strain were calculated by refining against the XRD patterns, and the elemental composition was obtained via energy dispersive X-ray analysis on single nanocrystals with TEM observations. The synthetic conditions—structure and composition—light emission relationships were discussed. The deficiency in calcium was the determining factor for the decreased light emission.

1. Introduction

Silicon-containing ternary and multinary (oxy)nitrides (or (oxo)nitridosilicates) are of technical importance. The well-known sialons are used as high-temperature structural materials.[1] Of great interest are the recent findings that some Eu^{2+} doped (oxy)nitrides are phosphors appropriate for use in white-light emitting diode devices: Ca- and Li-α-sialons (yellow),[2] $M_2Si_5N_8$ (orange-red),[3] $MSi_2O_2N_2$ (M = Ca, Sr, Ba; blue-yellow),[3,4] and $CaAlSiN_3$ (red).[5] Despite the significant potential in a variety of applications, the ternary and multinary (oxy)nitrides have been much less investigated than the oxide compounds of silicon, so information on their synthesis, properties, and applications is much less available than for the oxides.

Up to now, ternary and multinary (oxo)nitridosilicates have been widely synthesized using high-temperature processes. In one process, the solid-state reactions of silicon nitride (Si_3N_4) with other binary nitrides/oxides are used. Si_3N_4 is highly chemically and thermally stable; thus, the process usually requires rather high temperatures. By this process, the sialon[2] and the $CaAlSiN_3$[5] phosphors were synthesized at 1600–1800 °C. The temperatures could be lower for some materials, for example, $MSi_2O_2N_2$ (M = Ca, Sr, Ba; 1100–1400 °C).[4] In another process, the reactions of metals with silicon diimide are performed. By this route, the Schnick group has obtained a variety of novel ternary and multinary nitrides and oxynitrides

* Corresponding author. E-mail address: li.j.aa@m.titech.ac.jp or jinwangli@yahoo.com.
† Tokyo Institute of Technology.
‡ Present address: Department of Applied Chemistry, School of Science and Technology, Meiji University, 1-1-1 Higashimita, Tama-ku, Kawasaki 214-8571, Japan.
§ Present address: Department of Materials Science and Engineering, Shizuoka University, 3-5-1 Johoku, Hamamatsu 432-8561, Japan.
△ Mitsubishi Chemical Group Science and Technology Research Center, Inc.

(1) Cao, G. Z.; Metselaar, R. *Chem. Mater.* **1991**, *3*, 242.
(2) (a) Xie, R.-J.; Hirosaki, N.; Sakuma, K.; Yamamoto, Y.; Mitomo, M. *Appl. Phys. Lett.* **2004**, *84*, 5404. (b) Xie, R.-J.; Hirosaki, N.; Mitomo, M.; Takahashi, K.; Sakuma, K. *Appl. Phys. Lett.* **2006**, *88*, 101104.
(3) Mueller-Mach, R.; Mueller, G.; Krames, M. R.; Höppe, H. A.; Stadler, F.; Schnick, W.; Juestel, T.; Schmidt, P. *Phys. Status Solidi A* **2005**, *202*, 1727.
(4) Li, Y. Q.; Delsing, A. C. A.; de With, G.; Hintzen, H.T. *Chem. Mater.* **2005**, *17*, 3242.
(5) Uheda, K.; Hirosaki, N.; Yamamoto, Y.; Naito, A.; Nakajima, T.; Yamamoto, H. *Electrochem. Solid-State Lett.* **2006**, *9*, H22.
(6) See for example (a) Schnick, W.; Bettenhausen, R.; Götze, B.; Höppe, H. A.; Huppertz, H.; Irran, E.; Köllisch, K.; Lauterbach, R.; Orth, M.; Rannabauer, S.; Schlieper, T.; Schwarze, B.; Wester, F. *Z. Anorg. Allg. Chem.* **2003**, *629*, 902. (b) Schnick, W. *Int. J. Inorg. Mater.* **2001**, *3*, 1267. (c) Schnick, W.; Huppertz, H.; Lauterbach, R. *J. Mater. Chem.* **1999**, *9*, 289.

10.1021/cm071612m CCC: $40.75
Published on Web 03/06/2008

at ~1550–1650 °C in a radio frequency furnace,[6] including the above-mentioned $M_2Si_5N_8$[7] and $MSi_2O_2N_2$.[8] In still another, but less reported process, the carbothermal reduction and nitridation of oxides is used at 1400–1500 °C, for instance, for the synthesis of Ca−sialon[9] and $SrSi_5N_8$.[10] Very recently, $CaAlSiN_3$ was prepared via the self-propagating high-temperature (1450–1550 °C) synthesis from CaAlSi alloy in a radio frequency furnace.[11]

Low-temperature liquid processes for the nitride synthesis have advantages for energy savings, nanomaterials formation, and crystal growth at much lower pressures than the melt-growth method. Some binary nitrides have been synthesized via low-temperature liquid processes, for example, Si_3N_4 via the reaction between excess liquid silicon tetrachloride and magnesium nitride,[12] GaN from reactions under solvothermal conditions (in organic solvents[13] or supercritical ammonia)[14] or in a sodium flux.[15] Low-temperature syntheses for silicon-containing ternary and multinary nitrides are rarely reported. The synthesis in a sodium flux gained some success in this aspect. For example, $MSiN_2$ (M = Ca, Sr, Ba)[16] and $Ba_5Si_2N_6$[17] were obtained at 900–1100 °C and 750–850 °C, respectively.

We now report the synthesis of a multinary nitride, Eu-doped $CaAlSiN_3$, from CaAlSi alloy powder or its derived ammonometallates in ammonia at low temperatures (500–800 °C). This nitride is a red phosphor and was previously synthesized from binary nitrides at 1600–1800 °C.[5] We considered and confirmed the synthesis and crystallization of $CaAlSiN_3$ via the decomposition of metal amides in an ammonia solution, which is analogous to the oxide synthesis from hydroxides in water solutions, as shown below.

In ammonia solution, decomposing by releasing NH_3:

amide → imidoamide → more polymerized compounds → nitride

In water solution, decomposing by releasing H_2O:

hydroxide → oxyhydroxide → oxide

(Hereafter we refer to the amide and its partially polymerized compounds as ammonometallates.) The oxide synthesis in a water solution at low temperatures is a soft solution process.[18] Similarly, the nitride synthesis in an ammonia solution may be "softer" than the high-temperature processes. On the basis of the literature,[19] we have been able to directly synthesize ammonometallates from the CaAlSi alloy in ammonia−sodium amide ($NaNH_2$) solutions. Our samples obtained by the decomposition of ammonometallates were well-crystallized nanocrystals. This synthetic route may be able to produce a variety of forms (powders, films, single crystals) of multinary nitrides from nanostructures to large crystals. The significantly lower temperatures utilized in this method may allow the synthesis of other various nitrides that are inaccessible via high-temperature processes due to their low decomposition temperatures.

In a previous communication, we reported a well-crystallized, Eu-doped red-emitting $CaAlSiN_3$ product synthesized via this process.[20] In the present paper, we discuss the influence of the synthesis conditions, that is, pressure, temperature, heating rate, presence and absence of sodium amide, replacement of sodium amide with sodium azide, and use of presynthesized ammonometallates, on the composition, crystallinity, and photoluminescent properties of the products. It is interesting that $CaAlSiN_3$ can be synthesized in molten sodium amide even in an atmospheric ammonia flow.

2. Experimental Section

All operations for the syntheses were performed with the protection of a nitrogen or argon atmosphere. The CaAlSi alloy with a low concentration of Eu (composition $Ca_{0.992}Eu_{0.008}AlSi$) was made by melting stoichiometric amounts of the component metal blocks (Ca > 99.5%, Hitachi Alloy, Ltd., Japan; Al 99.999% and Si 99.999%, Kojundo Chemical Laboratory Co., Ltd., Japan; Eu > 99.0%, Mitsubishi Chemical Inc., Japan) on a water-cooled copper plate in a laboratory electric arc furnace, followed by quenching in an argon atmosphere. The alloy was ground into a powder (<50 μm) and then stored in nitrogen for the subsequent experiments. The particles of the ground alloy powder were irregular in shape. Most particles were a few micrometers in size, with some large ones up to 50 μm (Figure 1a). The CaAlSi alloy formed an intermetallic compound with an AlB_2 type structure (space group *P6/mmm*, Figure 1b).[21] A minor $CaAl_2Si_2$ phase and a minor unknown phase were also detected.

The synthetic experimental conditions are summarized in Table 1, and the nomenclature for the sample names is explained in the Table's footnote. For the synthesis in supercritical ammonia, the alloy powder (~0.1 g) was mixed with sodium amide (90%, Wako, Japan) at the molar ratio of Na/Ca = 5 and loaded into a bottom-sealed nickel tube (4 mm outer diameter, 0.125 mm thickness, 5 cm length) in a nitrogen-filled glovebox. The nickel tube was transferred into a vertically positioned superalloy pressure vessel (5 mm inner diameter, 20 cm length), which was then fully filled with anhydrous liquid ammonia (99.9%, Showa Denko, Japan) via condensation. A thermocouple was fixed to the surface of the pressure vessel at the position of the sample bottom, where the

(7) Schlieper, T.; Milius, W.; Schnick, W. *Z. Anorg. Allg. Chem.* **1995**, *621*, 1380.
(8) Höppe, H. A.; Stadler, F.; Oeckler, O.; Schnick, W. *Angew. Chem.* **2004**, *116*, 5656; *Angew. Chem., Int. Ed.* **2004**, *43*, 5540.
(9) Suehiro, T.; Hirosaki, N.; Xie, R.-J.; Mitomo, M. *Chem. Mater.* **2005**, *17*, 308.
(10) Piao, X.; Horikawa, T.; Hanzawa, H.; Machida, K. *Appl. Phys. Lett.* **2006**, *88*, 161908.
(11) Piao, X.; Machida, K.; Horikawa, T.; Hanzawa, H.; Shimorura, Y.; Kijima, N. *Chem. Mater.* **2007**, *19*, 4592.
(12) Zou, G.; Hu, B.; Xiong, K.; Li, H.; Dong, C.; Liang, J.; Qian, Y. *Appl. Phys. Lett.* **2005**, *86*, 181901.
(13) (a) Xie, Y.; Qian, Y.; Wang, W.; Zhang, S.; Zhang, Y. *Science* **1996**, *272*, 1926. (b) Sardar, K.; Rao, C. N. R. *Adv. Mater.* **2004**, *16*, 425.
(14) (a) Yoshikawa, A.; Ohshima, E.; Fukuda, T.; Tsujib, H.; Oshima, K. *J. Cryst. Growth* **2004**, *260*, 67. (b) Kagamitani, Y.; Ehrentraut, D.; Yoshikawa, A.; Hoshino, N.; Fukuda, T.; Kawabata, S.; Inaba, K. *Jpn. J. Appl. Phys., Part 1* **2006**, *45*, 4018. (c) Purdy, A. P. *Chem. Mater.* **1999**, *11*, 1648. (d) Purdy, A. P.; Case, S.; Muratore, N. *J. Cryst. Growth* **2003**, *252*, 136.
(15) (a) Yamane, H.; Shimada, M.; Clarke, S. J.; DiSalvo, F. J. *Chem. Mater.* **1997**, *9*, 413. (b) Yamada, T.; Yamane, H.; Iwatac, H.; Sarayama, S. *J. Cryst. Growth* **2006**, *286*, 496.
(16) Gál, Z. A.; Mallinson, P. M.; Orchard, H. J.; Clarke, S. J. *Inorg. Chem.* **2004**, *43*, 3998.
(17) Yamane, H.; Disalvo, F. J. *J. Alloys Compd.* **1996**, *240*, 33.
(18) Yoshimura, M. *J. Mater. Sci.* **2006**, *41*, 1299.
(19) (a) Levine, R.; Fernelius, W. C. *Chem. Rev.* **1954**, *54*, 449. (b) Bergstrom, F. W.; Fernelius, W. C. *Chem. Rev.* **1937**, *20*, 413. (c) Bergstrom, F. W.; Fernelius, W. C. *Chem. Rev.* **1933**, *12*, 43.
(20) Li, J.; Watanabe, T.; Wada, H.; Setoyama, T.; Yoshimura, M. *Chem. Mater.* **2007**, *19*, 3592.
(21) (a) Imai, M.; Nishida, K.; Kimura, T.; Abe, H. *Appl. Phys. Lett.* **2002**, *80*, 1019. (b) Sparta, K. M.; Mueller, R.; Merz, M.; Roth, G.; Adelmann, P.; Wolf, T. *Acta Crystallogr., Sect. B* **2006**, *62*, 710.

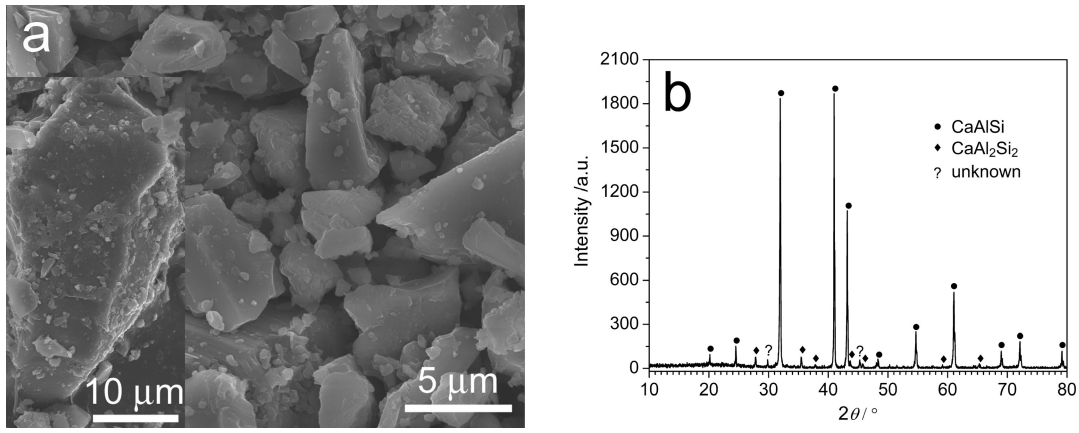

Figure 1. SEM images (a) and XRD pattern (b) of the starting alloy powder. The inset in part a shows some large particles (up to 50 μm) are present.

Table 1. Summary of Typical Experimental Data

sample[a]	Na/Ca ratio	heating conditions[b]	crystallized phases in the products[c]	$CaAlSiN_3$ size,[d] nm
		I. In 100 MPa Ammonia		
		1. Heated at a preset temperature (using ≥90% purity $NaNH_2$ and 99.9% purity NH_3)		
P4a	5.0	400 °C 20 h	$Ca(OH)_2$[e]	na
P4b	5.0	400 °C 65 h	$Ca(OH)_2$[e]	na
P5a	5.0	500 °C 20 h	$CaAlSiN_3 + Ca(OH)_2$	20
P5b	5.0	500 °C 65 h	$CaAlSiN_3 + Ca(OH)_2$	nc
P6a	5.0	600 °C 20 h	$CaAlSiN_3 + Ca(OH)_2$ + X	27
P6b	5.0	600 °C 66 h	$CaAlSiN_3 + Ca(OH)_2$	27
P4Na0	0.0	400 °C 20 h	similar to the starting alloy	na
P5Na0a	0.0	500 °C 20 h	$Ca(OH)_2$ + X	na
P5Na0b	0.0	500 °C 70 h	$CaAlSiN_3 + Ca(OH)_2 + CaCO_3$ + X	nc
P6Na0	0.0	600 °C 20 h	$CaAlSiN_3 + Ca(OH)_2 + CaCO_3$ + X	nc
		2. First held at 600 °C and then at 800 °C (using ≥90% purity $NaNH_2$ and 99.9% purity NH_3)		
P6-8	5.0	600 °C 23 h, 5 K/min, 800 °C 24 h	$CaAlSiN_3$ + AlN	27
P6-8Na0	0.0	600 °C 21 h, 5 K/min, 800 °C 21.5 h	$CaAlSiN_3$ + AlN + $Ca(OH)_2$ + Si	25
		3. First held at 400 °C and then heated at 0.1 or 1 K/min to 600–800 °C (using ≥90% purity $NaNH_2$ and 99.9% purity NH_3)		
P4-8r1	5.0	400 °C 20 h, 1 K/min, 800 °C 5 h	$CaAlSiN_3$ + AlN + $Ca(OH)_2 + CaCO_3$	33
P4-8r0.1	5.0	400 °C 20 h, 0.1 K/min, 800 °C 5 h	$CaAlSiN_3$ + AlN + CaO	44
P4-6r0.1	5.0	400 °C 20 h, 0.1 K/min, 600 °C 5 h	$CaAlSiN_3$ + AlN + $Ca(OH)_2$ + X	27
		4. First held at 400 °C and then heated at 0.1 K/min to 800 °C (using 99.99+% purity NaN_3 and 99.999% purity NH_3)		
P4-8r0.1NaN3	5.0	5 K/min, 400 °C 20 h, 0.1 K/min, 800 °C 5 h	$CaAlSiN_3$ + AlN	68
		5. Previously reported sample:[20] first held at 400 °C and then heated at 0.1 K/min to 800 °C (using 95% purity $NaNH_2$ and 99.999% purity NH_3)		
P4-8r0.1p95	5.0	400 °C 20 h, 0.1 K/min, 800 °C 5 h	$CaAlSiN_3$ + AlN + CaO	66
		II. In NH_3 Flow (using ≥90% purity $NaNH_2$ and 99.9% purity NH_3)		
NP4	5.0	3 K/min, 400 °C 20 h	X	na
NP5	5.0	3 K/min, 500 °C 20 h	$CaAlSiN_3 + Ca(OH)_2$	nc

[a] Nomenclature for the samples: $An_1(\text{-}n_2)(\text{r}n_3)(B)(s)$, where the items in the parentheses are optional, A = P (at 100 MPa) or NP (at 0.1 MPa), n_1 and n_2 indicate the holding temperatures (×100 °C), n_3 indicates the heating rate (K/min) after the formation of ammonometallates in the first stage of holding, B = Na0 (without using sodium), NaN3 (using NaN_3,) or p95 (using 95% $NaNH_2$), and s (= a, b, . . .) is for distinguishing different holding periods. [b] The heating rate was 20 K/min, if not otherwise indicated. The samples were naturally cooled down in the furnace. [c] XRD data, measured after washing with ethanol except for sample P6-8, which was measured after washing with water. $Ca(OH)_2$ and $CaCO_3$ were converted from CaO during storage in air. In some samples, Ni lines were also detected, which was due to the use of the Ni tube. [d] The sizes here were estimated only according to the broadening of the (002) XRD line. More precise calculation for both the size and the lattice strain was performed for three relatively well-crystallized samples via refinement against the XRD patterns (Table 2). [e] The as-synthesized samples P4a and P4b should contain ammonometallates as the major composition, which were hydrolyzed upon exposure to air. See the text for details. Abbreviations: na = not applicable, nc = not calculated, X = unknown phase(s).

center of a vertical tube furnace was placed. The upper part (~6 cm) of the pressure vessel, connected to other parts of the pressure system, was outside the furnace. Three groups of experiments were performed. In all the experiments, the pressure vessel was heated at 20 K/min from room temperature and, after the final heating step, naturally cooled down within a few hours to room temperature. For the first group of experiments (I.1 in Table 1), the pressure vessel was heated to a preset temperature (300–600 °C) and held for a specific time up to 70 h. This was to confirm the formation of the ammonometallates at 300−400 °C and to study the $CaAlSiN_3$ synthesis directly from the alloy at higher temperatures without presynthesizing the ammonometallates. In the second group (I.2 in Table 1), the pressure vessel was first held at 600 °C to allow the synthesis of $CaAlSiN_3$ and then increased at 5 K/min to 800 °C for a further reaction. The synthesis was not directly performed at 800 °C because of the significant decomposition of ammonia above 600 °C. In the third group of experiments (I.3 in Table 1), the pressure vessel was first held at 400 °C to allow full conversion of the alloy to ammonometallates and then slowly heated (0.1 or 1 K/min) to 600–800 °C to allow decomposition of the ammonometallates and crystallization of the $CaAlSiN_3$. In all experiments, the pressure was kept at around 100 MPa at 300–800 °C. An ammonia-releasing valve was used to reduce the pressure when necessary. After the pressure vessel was cooled to room temperature, the ammonia was fully released and the pressure vessel was opened to the air. A portion of the sample went out of the Ni tube and was contaminated by the corroded inner wall of the pressure vessel. The major portion of the sample that remained in the Ni tube was

washed with ethanol. Some samples were further washed with water or a 0.2 M HCl solution. *Warning: Care must be taken because the excess sodium amide and the sodium ammonometallates violently react with ethanol and water, especially with water. Sparkles were observed upon carefully removing the ammonometallates produced at 300–400 °C from the nickel tube in air.* After washing, the samples were dried in air at 80 °C.

For comparison, synthesis experiments without using sodium amide and under conditions similar to those of the first and second groups were performed for the alloy powder (~0.2 g; I.1 and I.2 in Table 1).

Experiments at atmospheric pressure were conducted in an alumina tube heated in a horizontal tube furnace. The mixture of the alloy powder and sodium amide was loaded in an alumina boat, which was then placed in the alumina tube. In an ammonia flow (1 l/min), the sample was heated at 20 K/min to 400–500 °C (II in Table 1). At 500 °C, sodium amide gradually evaporated, and thus higher temperatures were not used for the synthesis.

The above experiments resulted in samples with a significant oxide contamination. The oxygen could come from the adsorbed water on the inner walls of the system, which was impossible to completely remove by evacuating, and also from the ammonia (99.9%) and sodium amide (90%). To minimize the oxide contamination, an experiment using high-purity ammonia (99.999%, Showa Denko, Japan) and high-purity sodium azide (NaN_3, 99.99+%, Aldrich) instead of the sodium amide was conducted at 100 MPa to produce $CaAlSiN_3$ from presynthesized ammonometallates. Sodium azide first decomposes and then converts to sodium amide during heating in ammonia. To further reduce the concentration of oxygen in the sample, more of the CaAlSi alloy (0.315 g) was used in a long Ni tube (13 cm; sample P4-8r0.1NaN3 in I.4 of Table 1). After the synthesis, the sample remaining in the Ni tube had a sample height of around 6 cm from the bottom. Because of a large temperature gradient along the axis of the tube furnace, only the bottom part of the sample (~2 cm height, temperature difference within 20 °C), that is, the part of the sample at the center of the furnace where the thermocouple was placed, was used for the analysis.

The X-ray diffraction (XRD) analysis was conducted using a Model MXP3VA diffractometer (MAC Science, Japan. Cu Kα radiation with graphite monochromator) with a step size of 0.02° 2θ. A silicon standard was used to calibrate the instrumental line broadening. Simple size estimation using the (002) line (the position of this line is indicated in Figure 2 below) was conducted. The other intense peaks were significantly broader because they were closely overlapped lines. In this estimation, a slow scan at 0.5°/min (sample P4-8r0.1NaN3) or 0.1–0.2°/min (other samples) was performed for the 2θ range of 34–38°, the Cu $K\alpha_2$ lines were removed by using the software provided with the diffractometer, the resultant lines were fitted with the approximation of the Lorentzian shape, and the Scherrer equation was applied. The accuracy of the size estimation according to the uncertainty of the line fitting was less than 3 nm. A more precise analysis for the XRD data using Rietveld refinement with the program FullProf Suite[22] was performed for three representative samples that were better crystallized than the others. The data for the refinement were collected at 0.5°/min. The peak shape was described by the Thompson−Cox−Hastings pseudo-Voigt function, and the lattice parameters and size and lattice strain values at different directions were calculated. Because of the inexactly known elemental composition, notably of N and O, and the inadequate quality of the sample crystals (small size and large strain), as will be described later, the exact atomic coordinates could not be obtained in the refinement. Nevertheless, to reduce the uncertainty and to avoid divergence in the refinement arising from the severe overlapping of many close lines, structural information for defining the XRD profile is helpful; thus, the ideal composition of $CaAlSiN_3$ was applied, and its atomic coordinates[11] were input as the initial values. Scanning electron microscopy (SEM) observations were performed using a SEM S-4500 microscope (Hitachi, Japan). Transmission electron microscopy (TEM) and energy-dispersive X-ray (EDX) analyses were conducted on a JEOL JEM-2010F microscope (JEOL, Japan). Each EDX spectrum was recorded with the analyzed area limited on one single nanocrystal to avoid the influence of the possible contaminating phase(s). The materials used for the calibration in the quantitative calculation of the elements are CaAlSi alloy (the starting material; for Ca, Al, and Si), high-purity Si_3N_4 (O < 2.0%, C < 0.2%, Cl and Fe < 100 ppm, Al and Ca < 50 ppm, without detectable oxygen signal in its EDX spectrum; Ube Industries, Japan; for calibrating N), α-Al_2O_3 (99.99%, Sumitomo Chemical Co., Ltd., Japan; for calibrating O), and Na_2CO_3 (99.5%, Kanto Chemical Co., Inc., Japan; for calibrating Na; heated at 200 °C overnight in air before the use). The photoluminescence analysis was conducted using an LS 55 luminescence spectrometer (Perkin-Elmer) at an excitation wavelength of 460 nm.

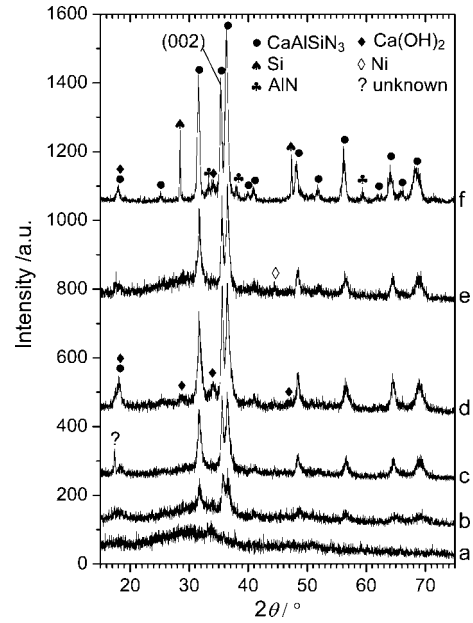

Figure 2. XRD patterns for samples obtained in 100 MPa ammonia: for samples starting with $NaNH_2$/CaAlSi = 5 and heated at 400 °C for 20 h, sample P4a (a), 500 °C for 20 h, sample P5a (b), 600 °C for 20 h, sample P6a (c), 600 °C for 66 h, sample P6b (d), 600 °C for 23 h and then 800 °C for 24 h, sample P6-8 (e), and the sample without using $NaNH_2$ and heated at 600 °C for 21 h then 800 °C for 21.5 h, sample P6-8Na0 (f). The samples were washed with ethanol (a−d) and both ethanol and water (e) and without washing (as synthesized) (f). The (002) line used for crystallite size estimation is indicated.

3. Results and Discussion

3.1. Ammonometallates Formation. In the early last century, it had been found that many metals, including calcium, aluminum, and silicon in our present system, reacted in molten alkali metal amides or its ammonia solution to form ammonometallates.[19] Silicon, a much less active element than calcium and aluminum, slowly reacts with molten sodium amide and potassium amide at 350–400 °C.[19a] Alloys are more active than their constituent elements, for

(22) Rodríguez-Carvajal, J. *Commission on Powder Diffraction (IUCr) Newsletter* **2001**, *26*, 12.

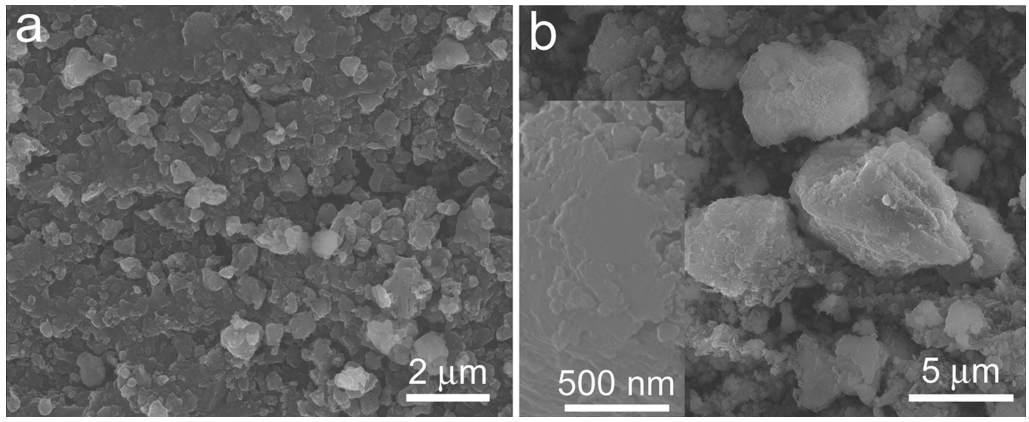

Figure 3. SEM images of ethanol-washed samples obtained in 100 MPa ammonia with $NaNH_2/CaAlSi = 5$, heated at 400 °C for 65 h, sample P4b (a), and 500 °C for 65 h, sample P5b (b). The inset in part b shows more details of the surface of the big particles at a higher magnification. Products at higher temperatures possess a morphology similar to the one at 500 °C.

example, during the nitridation of alkaline earth metal−silicon alloys.[16] Our results clearly showed that the black CaAlSi alloy powder was completely converted into white sodium ammonometallates after a reaction at 300–400 °C in a supercritical ammonia−sodium amide solution. (The lowest temperature that allows this conversion was not determined.) The products were highly moisture sensitive. When they were slowly removed from the nickel tube, these samples quickly released ammonia gas and became hot and sometimes generated sparkles. This is because the sodium ammonometallates were quickly hydrolyzed upon exposure to moisture. The XRD patterns of the samples after washing with ethanol showed only an amorphous phase and a small amount of $Ca(OH)_2$ (Figure 2a). Upon further washing with dilute HCl acid, these samples completely dissolved. Our present analysis conditions, however, do not allow a detailed analysis of the ammonometallate product without being exposed to air.

3.2. $CaAlSiN_3$ Formation without Presynthesis of Ammonometallates. The XRD patterns indicated that the direct reaction of the CaAlSi alloy in the 100 MPa ammonia−sodium amide solution at temperatures ≥ 500 °C led to formation of $CaAlSiN_3$, together with an amorphous phase and $Ca(OH)_2$ (which was later converted to $CaCO_3$) after washing in air (Table 1 and Figure 2). $Ca(OH)_2$ was formed during storage in air via the hydrolysis of the ammonometallates that remained undecomposed during the synthesis and hydrolysis of the CaO impurity produced in the synthesis because of oxygen contamination (see Figure 6c for CaO contamination). The sample produced at 500 °C (samples P5a and P5b) showed weak and broad XRD lines of $CaAlSiN_3$ (Figure 2b), indicating a low content and a small crystallite size. The mean crystallite size was ∼20 nm, estimated using the (002) line. Increasing the temperature to 600 °C resulted in more $CaAlSiN_3$ with a slightly larger size (∼27 nm), as indicated by the stronger and narrower XRD lines (Figure 2c). The increase in the reaction period, for example, from 20 h (sample P6a, Figure 2c) to 66 h (sample P6b, Figure 2d) at 600 °C, also led to more $CaAlSiN_3$ but without an increase in the crystallite size. After a reaction at 600 °C, further heating at 800 °C did not result in more $CaAlSiN_3$ or a larger size (sample P6-8, Figure 2e).

The fact that a prolonged reaction at 600 °C or further heating at higher temperatures up to 800 °C was not effective for the growth of the $CaAlSiN_3$ implies that $CaAlSiN_3$ is insoluble in the sodium amide−ammonia solution under the present conditions and thus cannot grow via a dissolution–crystallization process after formation. With regard to the solubility of the ammonometallates, it was reported that potassium ammonosilicate was insoluble in liquid ammonia,[19a] while sodium ammonoaluminate was soluble in a sodium amide−ammonia solution.[19c] No report was found about the solubility of alkaline metal ammonocalciates. Sodium ammonomagnesiate, which may have a solubility property similar to that of ammonocalciate, was reported to be hardly soluble in liquid ammonia.[19c] The detailed composition and structure of the ammonometallates in our system are unknown, but they could be multinary containing at least two metal elements including sodium. Accordingly, the sodium ammonometallates in our synthesis could be hardly soluble under the stated synthesis conditions and thus could not act as a solute for $CaAlSiN_3$ growth via a dissolution–crystallization process.

SEM images of the representative products are shown in Figure 3, and the morphology of the alloy powder is presented in Figure 1a. The SEM image of the ethanol-washed sample P4b obtained at 400 °C, which was indeed the hydrolysis product of the ammonometallates in air, showed a fine morphology completely different from the starting alloy powder. On the other hand, the products at 500 °C or higher temperatures, with $CaAlSiN_3$ formation, showed morphologies with a resemblance to the alloy powder; the shape of the alloy particles was maintained even after a long (65 h) reaction (sample P5b). This further supports the conclusion that $CaAlSiN_3$ is insoluble in the melts. It is clear that the reaction started on the surface of the alloy particles and proceeded inward. $CaAlSiN_3$, once formed, tended to stay at the original locations without growth because of its insolubility along with the very slow diffusion of atoms at such low temperatures. Consequently, the shape of the alloy particles was maintained by agglomeration of the $CaAlSiN_3$ crystallites (Figure 3b).

3.3. Effects of Sodium Amide. Without adding sodium amide, no apparent reaction between the alloy and the 100

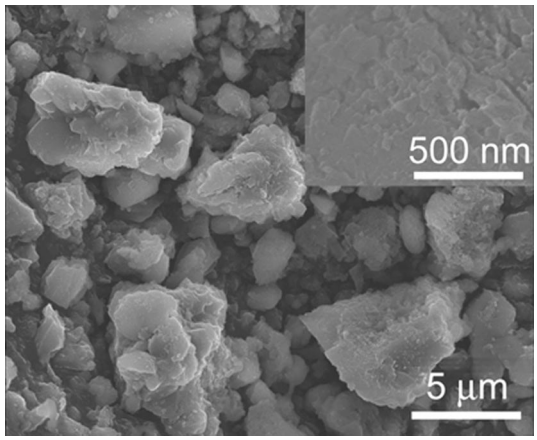

Figure 4. SEM images of an as-synthesized sample obtained in 100 MPa ammonia at 500 °C for 70 h, without using $NaNH_2$ (sample P5Na0b). The inset shows more details of the agglomerates at a higher magnification.

MPa ammonia was observed at 400 °C (sample P4Na0), according the unchanged black color and the XRD pattern. At 500 °C $CaAlSiN_3$ was not produced after a 20-h reaction (sample P5Na0a) but was produced after a prolonged (70 h) reaction (sample P5Na0b). At 600 °C, $CaAlSiN_3$ was obtained after a 20-h reaction (sample P6Na0). However, the reaction was rather incomplete and selective, as a significant amount of silicon remained unreacted. Further heating at 800 °C after the reaction at 600 °C failed to complete the conversion of silicon (sample P6-8Na0, Figure 2f). Thus, the addition of sodium amide is necessary to facilitate the synthesis and prevent selectivity of the reaction. With the presence of sodium amide, the sodium ammonometallates could form as intermediate products, which subsequently decomposed into $CaAlSiN_3$.

The mean crystallite size of the sample P6-8Na0 (Figure 2f) was ~25 nm, close to that of the sample obtained with sodium amide under similar conditions (sample P6-8, Figure 2e, ~27 nm). In other words, sodium amide did not effectively help the growth of $CaAlSiN_3$. This is more evidence that $CaAlSiN_3$ is insoluble in the ammonia−sodium amide solution. The XRD line intensities of $CaAlSiN_3$ obtained without sodium amide (Figure 2f) are, however, higher than those of the sample produced in the presence of sodium amide (Figure 2e). This could be attributed to the presence of a more amorphous phase in the latter sample, as shown in the XRD pattern. The amorphous phase was a result of the hydrolysis of the sodium ammonometallates that remained undecomposed during the synthesis. From a thermodynamic point of view, it is reasonable that some ammonometallates remained even after the reaction at 800 °C under the 100 MPa pressure, just like the fact that some supercritical ammonia does not decompose under such conditions because of chemical equilibrium.

SEM images (Figure 4) show that the products obtained without using sodium amide formed agglomerates with their shape resembling that of the alloy particles (Figure 1a). The mechanism for this shape retention is the same as the case shown in Figure 3b, as described above.

3.4. Synthesis under Atmospheric Pressure. Our experiments demonstrated that high pressure was unnecessary for the low-temperature formation of $CaAlSiN_3$ from the alloy in the presence of sodium amide. In flowing ammonia gas at atmospheric pressure, $CaAlSiN_3$ was synthesized at 500 °C (sample NP5, Figure 5). The alloy partially reacted at 400 °C, but no $CaAlSiN_3$ was formed (sample NP4). Sodium amide quickly evaporated at temperatures higher than 500 °C, and thus the synthesis was not performed at higher temperatures. As a result, better-crystallized $CaAlSiN_3$ was not obtained via a reaction at the higher temperatures in flowing ammonia gas. However, our results indicated that the synthesis of a higher-quality $CaAlSiN_3$ from the alloy at low pressures may be possible if the process is further improved, which could lead to a interesting low-temperature atmospheric-pressure synthesis and growth of $CaAlSiN_3$ and other nitrides.

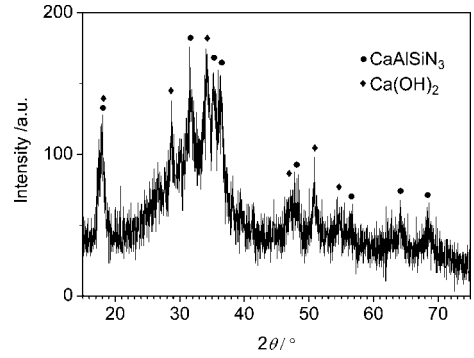

Figure 5. XRD pattern for the as-synthesized sample after a 20-h reaction in flowing ammonia gas at 500 °C, with $NaNH_2$:CaAlSi = 5 (sample NP5).

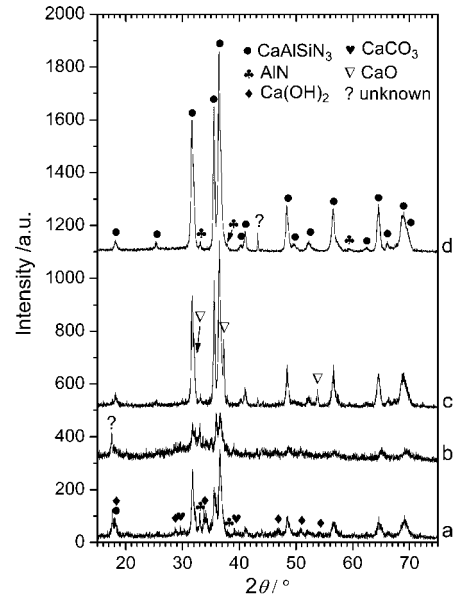

Figure 6. XRD patterns for samples obtained in 100 MPa ammonia with $NaNH_2$/CaAlSi = 5. The samples were first held at 400 °C for 20 h, and then slowly heated to the final temperatures and kept for 5 h. Heating rates above 400 °C and the final temperatures: (a) 1 K/min, 800 °C, sample P4-8r1, (b) 0.1 K/min, 600 °C, sample P4-6r0.1, and (c and d) 0.1 K/min, 800 °C, sample P4-8r0.1. Washed with (a−c) ethanol and (d) first ethanol and then 0.2 M HCl.

3.5. $CaAlSiN_3$ from Decomposition of Ammonometallates. As described above, the sodium ammonometallates were synthesized at 300–400 °C via the reaction of the CaAlSi alloy in an ammonia−sodium amide solution. Better-crystallized $CaAlSiN_3$ may be obtained via a controlled decomposition of the ammonometallates. Because $CaAlSiN_3$

did not grow via a dissolution–crystallization process, it is necessary to control the nucleation and growth of $CaAlSiN_3$ during the decomposition of the ammonometallates. The ammonometallates must be thermodynamically favored at low temperatures and be gradually converted into the nitride by successively losing ammonia and hydrogen with the increased temperature. By heating at a low rate, it is possible to slow down this process so as to achieve a low supersaturation level of the ammonometallates decomposition-derived species for the nucleation and growth of $CaAlSiN_3$. A lower supersaturation level can result in a lower crystal nucleation rate, leading to a preference of the growth of the crystals already formed over the formation of additional nuclei.

In 100 MPa ammonia, the alloy with sodium amide was first held at 400 °C for 20 h for the synthesis of the ammonometallates and then further slowly heated at 0.1 or 1 K/min to 600–800 °C to obtain $CaAlSiN_3$. Figure 6 is the XRD patterns of the products. The sample produced at the final temperature of 600 °C, even at a slow heating rate of 0.1 K/min, showed weak XRD lines of $CaAlSiN_3$ (sample P4-6r0.1, Figure 6b). Increasing the final temperature to 800 °C resulted in much stronger XRD lines (samples P4-8r1 and P4-8r0.1, Figure 6a and c). The heating rate also showed a significant effect. Decreasing the heating rate from 1 K/min (sample P4-8r1, Figure 6a) to 0.1 K/min (sample P4-8r0.1, Figure 6c) led to a significant increase in the XRD line intensities of the $CaAlSiN_3$. CaO, $Ca(OH)_2$, and $CaCO_3$ lines were also observed in the XRD patterns. CaO was found in the fresh ethanol-washed samples, which gradually converted into $Ca(OH)_2$ and $CaCO_3$ in sequence during the increased storage time in air. The CaO impurity was a result of oxygen contamination during the synthesis. To remove these impurities, these samples were further washed with acid (0.2 M HCl). Among these samples, the one obtained at a final temperature of 600 °C (sample P4-6r0.1) had the highest weight loss during acid washing, indicating the lowest conversion of ammonometallates to $CaAlSiN_3$, which was consistent with its weak XRD lines of $CaAlSiN_3$ (Figure 6b). The XRD pattern of the best-crystallized sample (sample P4-8r0.1, 0.1 K/min, final 800 °C) with the highest content of $CaAlSiN_3$ among these samples, after acid-washing, is shown in Figure 6d. The mean crystal size was ∼44 nm, larger than the compared samples P4-6r0.1 (∼27 nm) and P4-8r1 (∼33 nm) (Table 1), as estimated from the broadening of the (002) line. It contained a minor impurity of AlN along with an unidentified diffraction line that might be due to contamination from the container.

SEM images of the samples are shown in Figure 7. The sample P4-6r0.1, obtained at a final temperature of 600 °C, was not well crystallized, while samples produced up to 800 °C showed well-crystallized $CaAlSiN_3$ nanocrystals. The size and aspect ratio of the nanocrystals increased with a decrease in the heating rate from 1 K/min (sample P4-8r1, Figure 7e,f) to 0.1 K/min (sample P4-8r0.1, Figure 7c,d). Thus, the sample P4-8r1 showed mostly plate-like crystals with some bar-like ones, while the sample P4-8r0.1 showed predominantly bar-like crystals. The thicknesses of the crystals shown in the SEM images were consistent with the above values of the average sizes estimated from the XRD lines. SEM images taken both before and after the acid washing are presented as evidence that the plate- and bar-like crystals were $CaAlSiN_3$ instead of the washed away impurities.

3.6. Reducing Oxygen Contamination by Using Sodium Azide as the Sodium Source. All of the above-described products contained a significant amount of oxide impurities. As described in the Experimental Section, a purer sodium source and a larger amount of sample were used to minimize the concentration of the oxide contamination. Sodium amide is very moisture-sensitive and thus easily contaminated by oxygen because of the reaction with moisture. The use of a purer sodium amide (95%), the purest commercial product available from Aldrich, and a larger amount of sample resulted in a reduced but still XRD-detectable oxide impurity, as in the sample we presented in a previous communication.[20] In the further effort to reduce the oxygen contamination, high-purity sodium azide (99.99+%) was used instead of sodium amide along with a larger amount of sample (sample P4-8r0.1NaN3, see the Experimental Section for its preparation). In 100 MPa ammonia, sodium azide was found to decompose into sodium metal and nitrogen gas upon heating to 400 °C, as indicated by the pressure increase. The sodium metal could then react with ammonia to produce sodium amide under the experimental conditions. The sample was first heated at 400 °C for 20 h to complete the alloy → ammonometallates conversion and then slowly heated (0.1 K/min) to 800 °C and held for 5 h to produce $CaAlSiN_3$. The XRD pattern of the sample washed only with ethanol is shown in Figure 8. In contrast with the sample prepared with sodium amide and under the same heating conditions that showed a significant oxide contamination (sample P4-8r0.1, Figure 6c), no XRD lines indicating oxides were detected in Figure 8. The average crystallite size of the sample P4-8r0.1NaN3 was estimated to be ∼68 nm, according to the broadening of the (002) line, which is larger than sample P4-8r0.1 (∼44 nm, prepared with 90% pure sodium amide), and similar to the previously reported sample that was prepared with 95% pure sodium amide under the same conditions (∼66 nm).[20]

An SEM image of the sample P4-8r0.1NaN3, prepared with sodium azide, showed only plate-like crystals (Figure 9), different from the samples prepared with sodium amide that showed both plate-like and bar-like crystals (Figure 7). The reason for this will be discussed below. The thickness of the plates shown in the SEM image in Figure 9 is consistent with the value estimated from the XRD line broadening (68 nm), but the width is much larger (∼200–400 nm).

3.7. Photoluminescent Property. The photoluminescent emission spectra of the samples with the excitation of a blue light (λ = 460 nm) are shown in Figure 10. The samples show red emission centered at 630–644 nm. The emission intensity increases with using sodium (compare P6b and P6Na0, P6-8 and P6-8Na0), increasing synthesis temperature (compare, for example, P6b and P6-8, P4-6r0.1 and P4-8r0.1), and decreasing heating rate (compare P4-8r1 and P4-8r0.1); that is, the emission increases as the synthetic conditions change to more favor the formation of $CaAlSiN_3$.

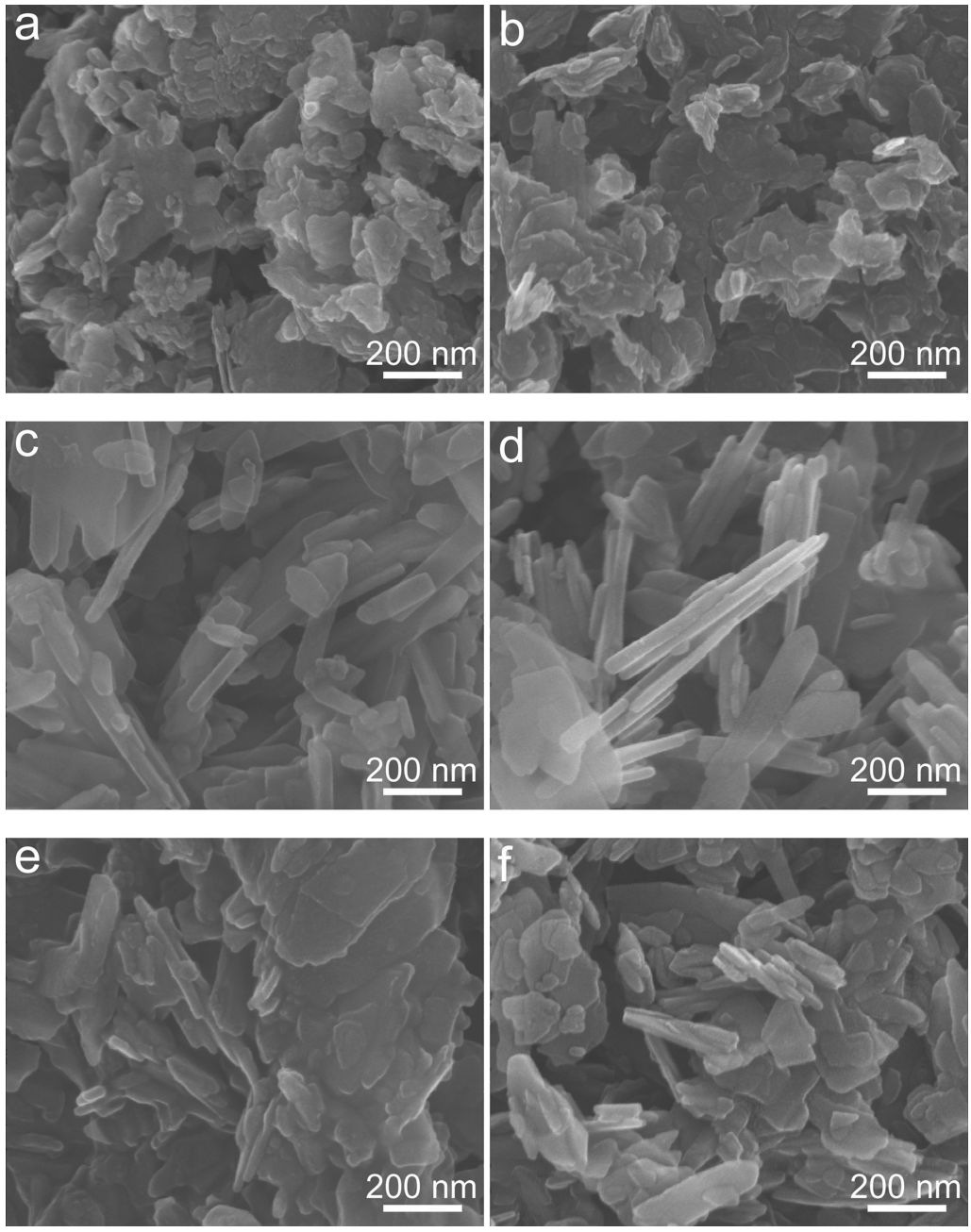

Figure 7. SEM images of samples obtained in 100 MPa ammonia with $NaNH_2$/CaAlSi = 5. The samples were first held at 400 °C for 20 h and then slowly heated to the final temperatures and kept for 5 h. Heating rates above 400 °C and the final temperatures: (a and b) 0.1 K/min, 600 °C, sample P4-6r0.1, (c and d) 0.1 K/min, 800 °C, sample P4-8r0.1, and (e and f) 1 K/min, 800 °C, sample P4-8r1. Washed with (a, c, and e) ethanol and (b, d, and f) first ethanol and then 0.2 M HCl.

This is, in general, consistent with the above-described XRD and SEM results.

We expected that the reduction of the oxide contamination could lead to a stronger photoluminescent emission. Unfortunately, the sample P4-8r0.1NaN3, which showed no oxide phases in the XRD pattern, did not emit a strong light as expected. The emission spectrum of the sample (P4-8r0.1p95, Table 1) that has been reported in our previous communication[20] and was prepared with 95% pure sodium amide under the same experimental conditions as the sample P4-8r0.1NaN3 is also presented in Figure 10 for comparison. In fact, the sample P4-8r0.1p95, which contained oxide impurity before washing with acid as indicated by the XRD spectrum, showed a light emission intensity 4.6 times higher than sample P4-8r0.1NaN3 (Figure 10b). The analyses in the next section will find out the reason.

3.8. Structural and Compositional Analyses of Three Representative Samples. Detailed structural and compositional analyses were performed for three representative samples that were better crystallized and showed stronger light emissions than the others. These three samples, namely, P4-8r0.1, P4-8r0.1NaN3, and P4-8r0.1p95, were prepared using different sodium sources (≥90% $NaNH_2$, 99.99+% NaN_3, and 95% $NaNH_2$, respectively) under the same temperature and pressure conditions (Table 1). They showed differences in both the intensity and the wavelength position (Figure 10). Their detailed analyses are helpful to elucidate the synthetic conditions—structure and composition—light emission relationships.

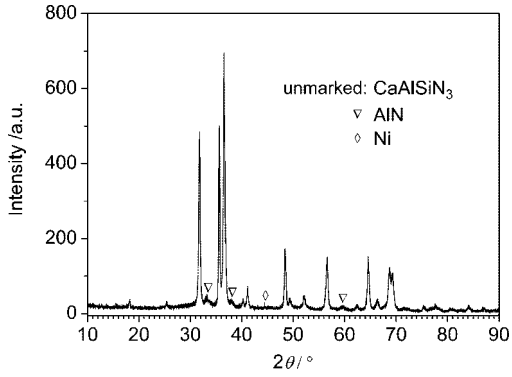

Figure 8. XRD pattern of the sample P4-8r0.1NaN3 obtained in 100 MPa ammonia with sodium azide being the sodium source ($NaN_3/CaAlSi = 5$). The sample was first held at 400 °C for 20 h and then heated at 0.1 K/min to 800 °C and kept for 5 h. It was only washed with ethanol.

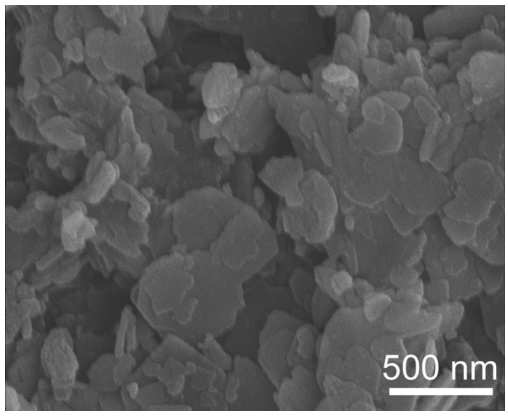

Figure 9. SEM image of the sample P4-8r0.1NaN3 as described in the caption of Figure 8.

The lattice parameters (orthorhombic, $Cmc2_1$, No. 36), crystallite size, and lattice strain obtained from the refinement of the XRD data are presented in Table 2, and a typical plot of the refinement results is shown in Figure 11. P4-8r0.1p95, the sample having the strongest light emission, shows the largest lattice cell with the cell parameters close to the previously reported values for samples from the high-temperature process,[5,11] while P4-8r0.1, which is the weakest in light emission, has significantly smaller lattice cell than the other two samples. This is because of their compositional difference as will be presented in the EDX analysis below.

The average and anisotropy size and strain values as well as the values along three selected directions resulted from the refinement are listed in Table 2. As expected according to the SEM observations, the size values showed significant anisotropy. The calculated sizes at different directions appear, however, all less than the length (P4-8r0.1 and P4-8r0.1p95) or width (P4-8r0.1NaN3) found in the electron microscopic observations (> 100 nm, see SEM in Figures 7and 9 and ref 20 and TEM in Figure 12 below). This could be caused by some contribution of the strain broadening in the size calculation because of the incomplete separation of the two broadenings. In fact, a size calculation from the XRD lines is reliable only for crystallites less than 100 nm. The average size values in Table 2 can be measurements of the crystal thicknesses, and other size values are useful only for relative comparison. The strain value is a measurement for the crystallinity, and P4-8r0.1 shows much higher strain values than the other two samples. Nevertheless, both size and strain are not the determining factor for the photoluminescent property in the present study because P4-8r0.1p95, which emits the strongest light, has the size and strain values between those of the other two samples.

TEM observations combined with the EDX analysis for elemental composition were performed for the three samples after acid wash. The morphologies shown in the TEM images (Figure 12) are consistent with the SEM observations. The high-resolution TEM images (insets in Figure 12) indicate clearly that the nanoparticles are single crystals. In the EDX analysis, each spectrum was recorded with the analysis area limited on one single crystal to exclude the influence from other possible contaminating phase(s). The atomic composition was calculated from the EDX data and normalized against the value of silicon, and the results are listed in Table 3. A reference $CaAlSiN_3$ sample (Mitsubishi Chemical), which was prepared via the high-temperature (1800 °C) process, was also analyzed, and the results are listed in the Table for comparison. The reference sample showed a large amount of oxygen ($O/Si = 0.63(17)$), which must be caused by the surface hydrolysis during storage in air. It is known that Ca_3N_2 is very moisture-sensitive, and AlN hydrolyzes easily in moist air at room temperature.[23] Thus, $CaAlSiN_3$, which contains both Ca−N and Al−N bonds, can also be hydrolyzed in contact with moisture and form an oxide surface layer like in the case of AlN.[24] The surface oxide layer is visible in the high-resolution TEM images (Figure 12). Because the hydrolysis changes the amount of anions, the resultant composition values for the metal elements are reliable, but those for oxygen and nitrogen can be different from the composition in the nitride lattice, especially for nanocrystals where the surface contribution is significant. The slight overestimation of the nitrogen values (over 3.0 and are expected to be less than 3.0 because of the presence of oxygen and the deficiency of Ca and Al) as indicated in some samples is attributed to the systematic error arising from the calibration of nitrogen.

As listed in Table 3, all samples show deficiency in Ca and Al. The deficiency of Ca and Al in the reference sample can be a result of evaporation of the metals at high temperatures (1800 °C). All samples from the low-temperature synthesis show the presence of sodium. Because the samples have been washed using acid, the sodium must be in the lattice of the nitride. Of the three samples, P4-8r0.1p95 showed the highest Ca content (0.74(9), and also a high Al value) that is the closest to the reference sample's (0.88(4)), while P4-8r0.1 possesses the lowest Ca (0.32(3)) and the highest Na (0.19(1)) contents. This coincides with the unit cell sizes presented above: P4-8r0.1p95 is the largest in the unit cell, and P4-8r0.1 is the smallest. Thus, the deficiency in Ca resulted in the shrinkage of the lattice. Poor crystallinity will be resulted if a metal is significantly deficient, as indicated by the rather larger strain values of P4-8r0.1. Accordingly, it is clear now that the decreased photoluminescent emission described above is predominantly a result of the deficiency in Ca. In consideration

(23) Li, J.; Nakamura, M.; Shirai, T.; Matsumaru, K.; Ishizaki, C.; Ishizaki, K. *J. Am. Ceram. Soc.* **2006**, *89*, 937.
(24) Li, J.; Matsumaru, K.; Ishizaki, C.; Ishizaki, K. *J. Am. Ceram. Soc.* **2006**, *89*, 2537.

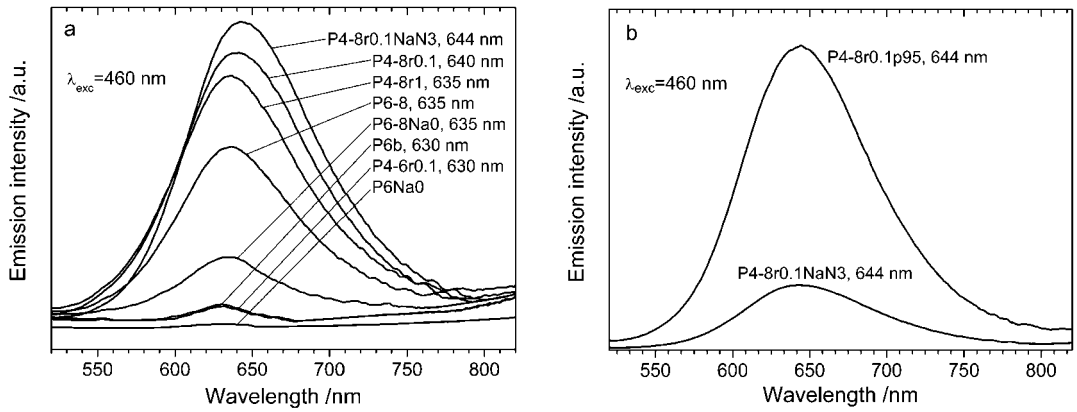

Figure 10. Emission spectra of the products at the excitation of a blue light ($\lambda = 460$ nm). The wavelength of each peak position is indicated after the sample name. The emission of sample P4-8r0.1p95 is much stronger than those of other samples and is presented at a contracted scale in part b. The spectrum of sample P4-8r0.1NaN3 is shown in both part a and part b for relative comparison.

Table 2. Results of Rietveld Refinement for the Size and Lattice Strain of Three Samples

sample	P4-8r0.1	P4-8r0.1p95	P4-8r0.1NaN3
	Lattice Parameters		
a, Å	9.651(3)	9.7676(8)[a]	9.763(1)
b, Å	5.6178(6)	5.6440(1)[a]	5.6325(5)
c, Å	5.0197(8)	5.0529(1)[a]	5.0412(4)
Volume, Å^3	272.17(10)	278.56(2)[a]	277.22(5)
	Apparent Size, Å		
average	215	289	372
anisotropy	103	107	151
[100]	244	499	534
[010]	141	354	270
[001]	470 [113][b]	497 [024][b]	701
	Maximum Strain/10^{-4}		
average	48.7	23.6	18.0
anisotropy	17.9	9.2	6.3
[100]	61.8	34.8	17.1
[010]	71.0	38.0	14.6
[001]	42.7 [113][b]	18.3 [024][b]	22.6
	Agreement Factors		
R_p	15.4	14.0	15.3
R_{wp}	20.7	20.7	22.1
R_{exp}	16.58	19.35	18.89
χ^2	1.56	1.14	1.37

[a] These lattice parameters are slightly different from the previously reported ones in ref 20 where another simpler program was used. As a result of the significant overlapping of many XRD lines, the present values from the Rietveld refinement of the whole XRD data should be more reliable. [b] The value along [001] is unavailable because of the resolution limit in the refinement.

that the Eu dopant occupies the Ca sites to give the light-emitting feature, it is rather evident that the Ca concentration plays a key role in determining the photoluminescent emission.

$NaSi_2N_3$ (space group $Cmc2_1$, $a = 9.468(1)$ Å, $b = 5.502(1)$ Å, $c = 4.878(5)$ Å, from No. 48-1431 in PDF-2 database) has the same structure and close lattice parameters with $CaAlSiN_3$, implying they may form solid solutions. The presence of sodium in the lattice of our samples indicates they are in fact such solutions. Si_2N_2O (space group $Cmc2_1$, $a = 8.868(6)$ Å, $b = 5.497(9)$ Å, $c = 4.854(2)$ Å, from No. 47-1627 in PDF-2 database), having also the same structure but smaller lattice parameters, may also form solid solutions to some extent as a result of oxygen contamination. Unfortunately, we cannot separate the contributions from the surface and the nitride lattice for the oxygen data in Table 3, though a large oxygen value of P4-8r0.1 (0.71(3)) may indicate its high concentration in the sample's lattice.

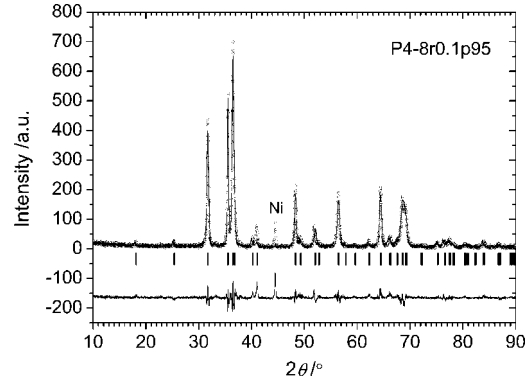

Figure 11. The results of the Rietveld refinement of the sample P4-8r0.1p95. Observed (circle), calculated (line), and difference (bottom line) profiles are shown. Tick marks indicate Bragg positions.

It is unclear why the use of the high-purity NaN_3 (sample P4-8r0.1NaN3) did not result in an improved structure and light-emitting property. NaN_3 was converted to $NaNH_2$ below 400 °C and thus was expected to play the same role in the reaction as the directly added $NaNH_2$. A possible reason is that a small amount of oxygen, as in the case of P4-8r0.1p95, facilitated the crystallization of the targeted nitride through formation of some intermediates that provided the media for quicker diffusion of some elements. Such media also led to the growth of elongated crystals as shown by the samples with $NaNH_2$ as a starting material. However, at a high level of oxygen in the system, as in the case of P4-8r0.1 that synthesized with a low-purity (90%) $NaNH_2$, a significant amount of Ca formed the CaO phase (indicated by XRD), resulting in very low concentration of Ca in the nitride.

On the basis of these analyses, one may also explain the shift of the emission wavelengths as presented in Figure 10. The shift of emission to shorter wavelengths can arise from two changes. The first is the decrease of the Eu dopant level,[5,11] and the second is the increase of oxygen in the lattice.[11] The decreasing dopant level also results in a reduction of the emission intensity in our concentration range of Eu.[5,11] A low Ca concentration may imply a low Eu level. Thus, the shift of the emission from 644 nm of P4-8r0.1NaN3 to 640 nm of P4-8r0.1 could be caused by the changes in both the Eu (as implied by the rather lower Ca content in P4-8r0.1) and the oxygen (low purity $NaNH_2$ (90%) was used for the preparation of P4-

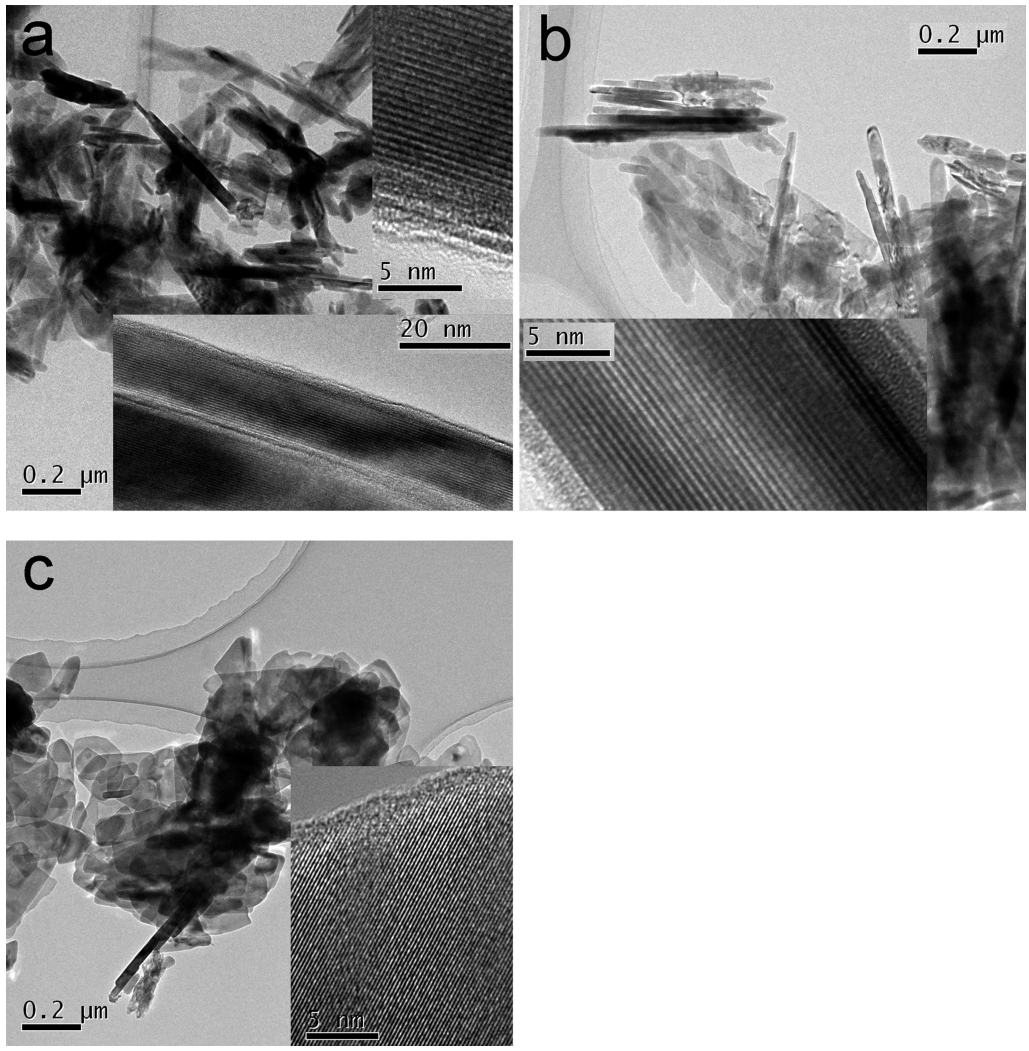

Figure 12. TEM images of the samples P4-8r0.1 (a), P4-8r0.1p95 (b), and P4-8r0.1NaN3 (c). The insets are the high-resolution images of the nanocrystals.

Table 3. Atomic Compositions of Three Samples and a Reference Sample Produced via the High-Temperature Process. [a]

sample	Ca	Na	Al	Si	N	O
P4-8r0.1	0.32(3)	0.19(1)	0.82(7)	1.0	3.4(1)	0.71(3)
P4- 8r0.1p95	0.74(9)	0.11(2)	0.79(3)	1.0	2.8(9)	0.29(10)
P4-8r0.1NaN3	0.54(10)	0.10(1)	0.62(7)	1.0	3.4(1)	0.34(6)
reference	0.88(4)	nd[b]	0.85(3)	1.0	3.3(3)	0.63(17)

[a] The compositions are calculated from EDX data for single nanocrystals and normalized against the value of silicon. [b] nd = not detectable.

8r0.1) concentrations. The shift between P4-8r0.1 and P4-8r1 and between P6-8 and P6b might arise from decreased Eu dopant levels in the low-emission samples.

4. Conclusions

Eu-doped $CaAlSiN_3$ can be synthesized via the reaction of the CaAlSi alloy containing the Eu dopant with ammonia at 500–800 °C, that is, ≥1000 °C lower than the conventional synthesis methods. The presence of sodium amide facilitates the production of $CaAlSiN_3$ and prevents the presence of unreacted silicon, which could be due to the formation of sodium ammonometallates as intermediates. The synthesis may be conducted even under atmospheric pressure, but the crystallinity is low. The reactions of the alloy in the presence of sodium amide in pressurized ammonia (100 MPa) at 500–800 °C give poorly crystallized $CaAlSiN_3$ even after a long holding time. This is because $CaAlSiN_3$ is insoluble in the ammonia−sodium amide solution under the present conditions. The decomposition of the presynthesized sodium ammonometallates by slow heating up to 800 °C leads to well-crystallized plate- and bar-like $CaAlSiN_3$ nanocrystals. The products emit red light at a blue excitation. The use of sodium azide instead of sodium amide as the sodium source can significantly reduce oxide contamination but failed to improve the light emitting property. The deficiency of calcium is the dominating reason for the decreased light emission of the samples. Some sodium entered into the nitride lattice. The replacement of sodium by potassium that has a larger atomic size may result in purer samples without the incorporation of the alkali metal. Larger crystals may be grown by further optimizing the reaction conditions. This synthesis route has a significant potential to be applied to other multinary nitrides.

Acknowledgment. We are thankful for the partial financial support from NEDO (New Energy and Industrial Technology Development Organization), Japan.

CM071612M